11th World Congress on Computational Mechanics (WCCM XI)
5th European Conference on Computational Mechanics (ECCM V)
6th European Conference on Computational Fluid Dynamics (ECFD VI)
E. Oñate, J. Oliver and A. Huerta (Eds)

ANALYSIS OF CRACKED MODEL UNDER FINITE-STRAIN ELASTOPLASTICITY USING PARTITIONED COUPLING METHOD

YASUNORI YUSA*AND SHINOBU YOSHIMURA‡

*,‡Department of Systems Innovation, School of Engineering, The University of Tokyo
7-3-1 Hongo, Bunkyo-ku, Tokyo 113-8656, Japan
*e-mail: yusa@save.sys.t.u-tokyo.ac.jp, web page: http://save.sys.t.u-tokyo.ac.jp/~yusa/
‡e-mail: yoshi@sys.t.u-tokyo.ac.jp, web page: http://save.sys.t.u-tokyo.ac.jp/

Key words: Large Deformation, Fracture Mechanics, Finite Element Method, Iterative Method

Abstract. Analyzing a cracked model under finite-strain elastoplasticity is helpful to evaluate structural integrity when a disaster occurs. Strongly nonlinear phenomena are observed near the crack, whereas nonlinearity far from the crack is relatively weak. We have been developing a partitioned coupling method to solve such problems efficiently. In the method, a whole analysis model is decomposed into two non-overlapped domains, i.e. local and global domains. The two domains are analyzed separately and alternately using an iterative solution technique, and finally a converged solution is obtained. As a benchmark, a cylindrical specimen model with a through-wall notch subjected to torsional loading was analyzed. The computed value of torque agreed well with that of a conventional FEM solver. Partitioned coupling was successfully converged in several iterations at every incremental step. The partitioned coupling approach did not degrade the convergence property of Newton–Raphson method. In addition, Newton–Raphson's iteration counts on the global mesh calculation were only a few because plasticity was not considered there. It is clearly demonstrated that one can utilize two different nonlinear solvers that work together using the partitioned coupling method to solve a problem in which remarkable nonlinearity occurs in a local region.

1 INTRODUCTION

Recently disasters such as earthquakes and tsunamis have been actively studied, especially after the Great East Japan Earthquake in March 2011. A structure in such disasters can be modelled as a finite element model with boundary conditions of large displacement and/or strong loading. When a crack is generated in the structure a priori due to fatigue or stress corrosion cracking, the crack would cause severe fracture during the disaster.

Analyzing a cracked model under finite-strain elastoplasticity is helpful for assessing such a problem. There is an issue in analyzing a real structure of complicated shape with cracks. Strongly nonlinear phenomena are observed near the crack, whereas nonlinearity far from the crack is relatively weak. When solving such a problem with the conventional FEM, a large portion far from the crack whose nonlinearity still remains weak has to be analyzed by a powerful nonlinear solver. To solve such a problem more efficiently, we have been studying a partitioned coupling method [1,2]. In the method, a whole analysis model is decomposed into two non-overlapped domains, i.e. local and global domains. The two domains are analyzed separately and alternately under assumed boundary conditions on the global–local interface. The assumed boundary conditions are updated by an iterative solution technique, and a converged solution is finally obtained. Two different solvers can be utilized for the local domain and for the global one, respectively.

In this paper, the partitioned coupling method is applied to a cracked model with finite-strain elastoplasticity. The local domain is modelled as a large-deformation elastoplastic body, while the global domain is modelled as a large-deformation elastic one. A computed result is compared with that of a conventional FEM solver.

2 METHODS

2.1 Partitioned Coupling Method

A whole analysis model is decomposed into two non-overlapped domains, as shown in Fig. 1. Since the two domains are analyzed separately in a partitioned coupling method, both geometrical compatibility and force equilibrium on the global–local interface are not satisfied in general. They however become satisfied by the iterative solution technique. An analysis on the local domain, Ω^L, is represented as

$$\boldsymbol{f}_\Gamma^{(k+1)} = L\left(\boldsymbol{u}_\Gamma^{(k)}\right) \tag{1}$$

and an analysis on the global domain, Ω^G, is represented as

$$\tilde{\boldsymbol{u}}_\Gamma^{(k+1)} = G\left(\boldsymbol{f}_\Gamma^{(k+1)}\right). \tag{2}$$

k is an iteration step. $\boldsymbol{u}_\Gamma$ is a displacement vector on the global–local interface, Γ, and $\tilde{\boldsymbol{u}}_\Gamma$ is a predicted displacement vector on Γ. $\boldsymbol{f}_\Gamma$ is a force vector on Γ. L is a function in which a local analysis is performed under an enforced displacement boundary condition, $\boldsymbol{u}_\Gamma$, on Γ, and a minus of a reaction force vector, $\boldsymbol{f}_\Gamma$, is returned. G is also a function in which a global analysis is performed under an external force boundary condition, $\boldsymbol{f}_\Gamma$, on Γ, and a displacement vector, $\boldsymbol{u}_\Gamma$, is returned. These functions themselves would be nonlinear owing to plasticity, finite strain and so forth. They are to be solved by Newton–Raphson method. From Eq. (1) and Eq. (2),

$$\tilde{\boldsymbol{u}}_\Gamma^{(k+1)} = G\left(L\left(\boldsymbol{u}_\Gamma^{(k)}\right)\right) \tag{3}$$

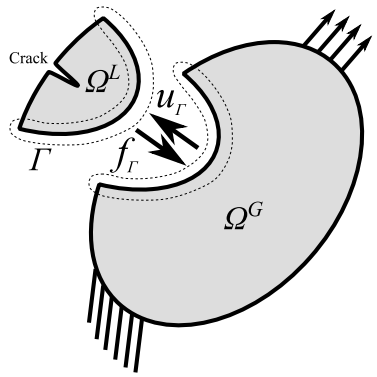

Figure 1: Decomposed analysis model and assumed boundary conditions on the global–local interface.

is obtained. A residual vector, R, is now defined as a function of

$$R\left(\boldsymbol{u}_{\boldsymbol{\Gamma}}\right) \equiv \boldsymbol{u}_\Gamma - G\left(L\left(\boldsymbol{u}_\Gamma\right)\right). \tag{4}$$

When geometrical compatibility on the global–local interface is satisfied, the residual should vanish as

$$R\left(\boldsymbol{u}_\Gamma\right) = \mathbf{0}. \tag{5}$$

This nonlinear equation is to be solved by an iterative solution algorithm. It is checked numerically with a tolerance, τ, as

$$\frac{\left\|R\left(\boldsymbol{u}_\Gamma\right)\right\|}{\left\|G\left(L\left(\boldsymbol{u}_\Gamma\right)\right)\right\|} \leq \tau \tag{6}$$

in the present study. In addition, force equilibrium also becomes satisfied when geometrical compatibility is satisfied at the k-th iteration step as

$$R\left(\boldsymbol{u}_\Gamma^{(k)}\right) = \boldsymbol{u}_\Gamma^{(k)} - G\left(L\left(\boldsymbol{u}_\Gamma^{(k)}\right)\right) = \mathbf{0}. \tag{7}$$

From this equation,

$$\boldsymbol{u}_\Gamma^{(k)} = G\left(L\left(\boldsymbol{u}_\Gamma^{(k)}\right)\right) \tag{8}$$

is obtained. The function of L is applied to both sides and then Eq. (1) is used.

$$\boldsymbol{f}_\Gamma^{(k+1)} - L\left(G\left(\boldsymbol{f}_\Gamma^{(k+1)}\right)\right) = \mathbf{0} \tag{9}$$

is finally derived. The left side of this equation is a force-based residual vector, whose form is similar to Eq. (4).

In the present study, limited-memory Broyden method [2, 3] is adopted to solve Eq. (5). The limited-memory Broyden method is a quasi-Newton method and satisfies secant condition:

$$\boldsymbol{B}^{(k+1)}\boldsymbol{s}^{(k)} = \boldsymbol{r}^{(k+1)} - \boldsymbol{r}^{(k)}. \tag{10}$$

$\boldsymbol{B}$ is an approximate Jacobian matrix,

$$\boldsymbol{s}^{(k)} \equiv \boldsymbol{u}_{\Gamma}^{(k)} - \boldsymbol{u}_{\Gamma}^{(k-1)} \tag{11}$$

is a search direction vector, and

$$\boldsymbol{r}^{(k+1)} \equiv R\left(\boldsymbol{u}_{\Gamma}^{(k)}\right) \tag{12}$$

is a residual vector. Broyden updating formula is here defined as

$$\boldsymbol{B}^{(k+1)} = \boldsymbol{B}^{(k)} + \frac{\boldsymbol{r}^{(k+1)}\boldsymbol{s}^{(k)\mathrm{T}}}{\left\|\boldsymbol{s}^{(k)}\right\|^2}. \tag{13}$$

Using Sherman–Morrison formula:

$$\left(\boldsymbol{M} + \boldsymbol{u}\boldsymbol{v}^{\mathrm{T}}\right)^{-1} = \left(\boldsymbol{I} - \frac{\boldsymbol{M}^{-1}\boldsymbol{u}}{1 + \boldsymbol{v}^{\mathrm{T}}\boldsymbol{M}^{-1}\boldsymbol{u}}\boldsymbol{v}^{\mathrm{T}}\right)\boldsymbol{M}^{-1}, \tag{14}$$

where $\boldsymbol{M}$ is an invertible matrix, and $\boldsymbol{u}$ and $\boldsymbol{v}$ are vectors whose size is the same as the matrix size, one can derive

$$\boldsymbol{s}^{(k+1)} \equiv -{\boldsymbol{B}^{(k+1)}}^{-1}\boldsymbol{r}^{(k+1)} = \frac{\boldsymbol{p}^{(k+1,k)}}{1 - \dfrac{\boldsymbol{s}^{(k)\mathrm{T}}\boldsymbol{p}^{(k+1,k)}}{\left\|\boldsymbol{s}^{(k)}\right\|^2}} \tag{15}$$

and

$$\boldsymbol{p}^{(k+1,i+1)} \equiv -{\boldsymbol{B}^{(i+1)}}^{-1}\boldsymbol{r}^{(k+1)} = \boldsymbol{p}^{(k+1,i)} + \frac{\boldsymbol{s}^{(i)\mathrm{T}}\boldsymbol{p}^{(k+1,i)}}{\left\|\boldsymbol{s}^{(i)}\right\|^2}\boldsymbol{s}^{(i+1)}. \tag{16}$$

A dense matrix, $\boldsymbol{B}$, is eliminated in above equations, so that this method does not require a large amount of memory. The algorithm of the limited-memory Broyden method is summarized as follows.

$\boldsymbol{s}^{(0)} \leftarrow -{\boldsymbol{B}^{(0)}}^{-1}\left(\boldsymbol{u}_{\Gamma}^{(-1)} - G\left(L\left(\boldsymbol{u}_{\Gamma}^{(-1)}\right)\right)\right)$
$\boldsymbol{u}_{\Gamma}^{(0)} \leftarrow \boldsymbol{u}_{\Gamma}^{(-1)} + \boldsymbol{s}^{(0)}$
$k \leftarrow 0$
while $\left\|\boldsymbol{r}^{(k)}\right\| \Big/ \left\|\tilde{\boldsymbol{u}}_{\Gamma}^{(k)}\right\| > \tau$ **do**
  $\tilde{\boldsymbol{u}}_{\Gamma}^{(k+1)} \leftarrow G\left(L\left(\boldsymbol{u}_{\Gamma}^{(k)}\right)\right)$
  $\boldsymbol{r}^{(k+1)} \leftarrow \boldsymbol{u}_{\Gamma}^{(k)} - \tilde{\boldsymbol{u}}_{\Gamma}^{(k+1)}$
  $\boldsymbol{p}^{(k+1,0)} \leftarrow -{\boldsymbol{B}^{(0)}}^{-1}\boldsymbol{r}^{(k+1)}$
  for $i \leftarrow 0$ to $k-1$ **do**
    $\boldsymbol{p}^{(k+1,i+1)} \leftarrow \boldsymbol{p}^{(k+1,i)} + \dfrac{\boldsymbol{s}^{(i)\mathrm{T}}\boldsymbol{p}^{(k+1,i)}}{\left\|\boldsymbol{s}^{(i)}\right\|^2}\boldsymbol{s}^{(i+1)}$

end for

$$\boldsymbol{s}^{(k+1)} \leftarrow \boldsymbol{p}^{(k+1,k)} \Big/ \left(1 - \frac{\boldsymbol{s}^{(k)\mathrm{T}}\boldsymbol{p}^{(k+1,k)}}{\left\|\boldsymbol{s}^{(k)}\right\|^2}\right)$$

$$\boldsymbol{u}_\Gamma^{(k+1)} \leftarrow \boldsymbol{u}_\Gamma^{(k)} + \boldsymbol{s}^{(k+1)}$$

$$k \leftarrow k+1$$

end while

This iteration is conducted at every incremental step. An initial guess, $\boldsymbol{u}_\Gamma^{(-1)}$, is zerofilled at the first incremental step, or filled with a previous converged solution, $\boldsymbol{u}_\Gamma^{(k+1)}$, at other incremental steps. An initial inverse approximate Jacobian matrix, $\boldsymbol{B}^{(0)^{-1}}$, is a user-defined parameter, which is determined to be a diagonal matrix whose diagonal entries are 0.1 in the present study.

2.2 Finite-strain Elastoplasticity Modelling

A hyperelasticity-based multiplicative decomposition model [4] is employed to represent finite-strain elastoplasticity in the present study. A deformation gradient tensor, $\boldsymbol{F}$, is assumed to be decomposed into an elastic component, $\boldsymbol{F}^e$, and a plastic one, $\boldsymbol{F}^p$, as

$$\boldsymbol{F} = \boldsymbol{F}^e\boldsymbol{F}^p \tag{17}$$

in the model. A constitutive equation of the Hencky model is described as

$$\boldsymbol{\tau} = \mathbb{C}^e : \boldsymbol{\varepsilon}^e = \mathbb{C}^e : \ln \boldsymbol{V}^e, \tag{18}$$

where $\boldsymbol{\tau}$ is Kirchhoff stress, $\mathbb{C}$ is a stiffness tensor, $\boldsymbol{\varepsilon}$ is Hencky strain and $\boldsymbol{V}$ is a left stretch tensor. Von Mises criterion and isotropic hardening is employed. Radial return method and a consistent tangential stiffness tensor is used in Newton–Raphson method.

3 BENCHMARK PROBLEM

A cylindrical specimen model with a 60-deg circumferential notch subjected to torsional loading was analyzed by the developed partitioned coupling solver and a conventional FEM solver. Dimension parameters are described in Fig. 2. Employed material parameters are Young's modulus of 203 GPa, Poisson's ratio of 0.3, initial yield stress, τ_{y_0}, of 300 MPa, and a stress–strain curve of

$$\bar{\tau} = \begin{cases} \tau_{y_0} + H'\bar{\varepsilon}^p & (\bar{\varepsilon}^p < \varepsilon_0^p) \\ \tau_{y_0} + F\left(\bar{\varepsilon}^p - \varepsilon_0^p\right)^n & (\bar{\varepsilon}^p \geq \varepsilon_0^p) \end{cases} \tag{19}$$

where $\varepsilon_0^p = 0.02447$, $H' = 408.6$ MPa, $F = 1123.4$ MPa and $n = 0.6846$. $\bar{\tau}$ is yield stress and $\bar{\varepsilon}^p$ is equivalent plastic strain. Decomposed mesh of the model is shown in Fig. 3. When solving with the partitioned coupling solver, finite-strain elastoplasticity is considered on the local mesh, while finite-strain elasticity is considered on the global one. When solving with the conventional FEM solver, finite-strain elastoplasticity is considered

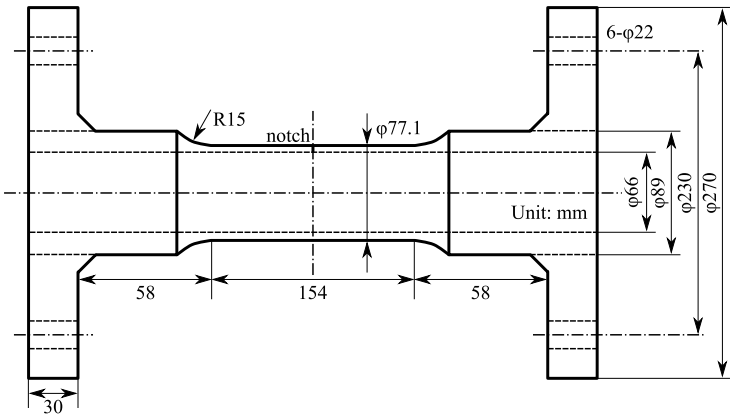

Figure 2: Dimension parameters of the cylindrical specimen model.

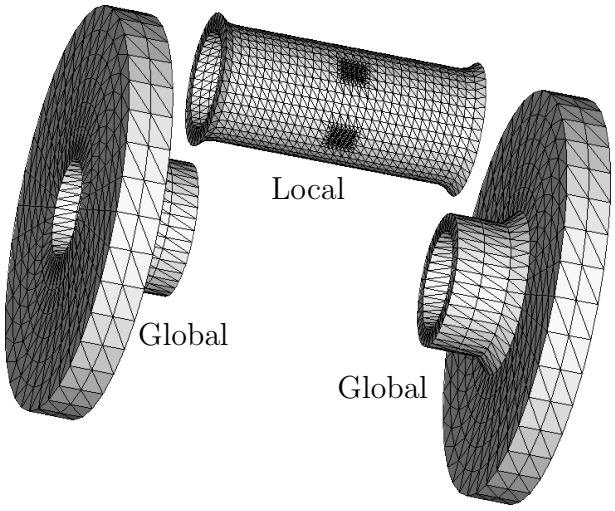

Figure 3: Decomposed mesh of the cylindrical specimen model.

on the whole mesh. Isoparametric quadratic tetrahedral elements are employed. Numbers of elements, nodes and degrees of freedom (DOFs) of the global mesh are 6,480, 11,952 and 35,856, respectively. Those of the local mesh are 12,852, 23,115 and 69,345, respectively. Numbers of nodes and DOFs on the global–local interface are 432 and 1,296, respectively. One side of the cylinder is constrained, while the other side is constrained in the axial direction and enforced with torsional displacement. The applied torsional displacement is varied gradually by 0.05 deg from 0 to 30 deg. The total number of incremental steps is 600. The tolerance of Newton–Raphson method is set as 10^{-6}, while that of the partitioned coupling method is set as 10^{-3}.

The computed result of equivalent plastic strain at a torsional angle of 30 deg is shown

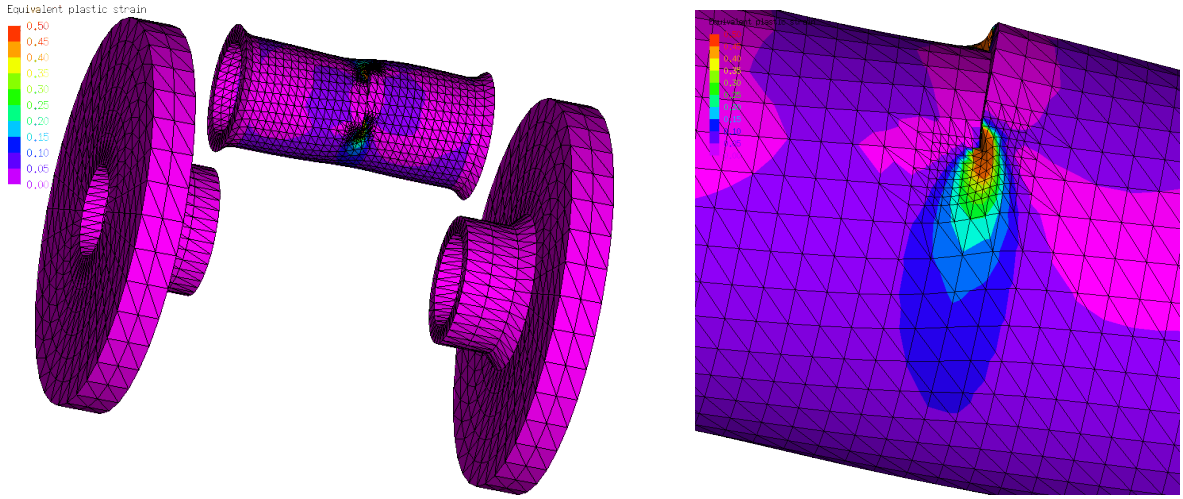

Figure 4: Equivalent plastic strain distribution of the cylindrical specimen model.

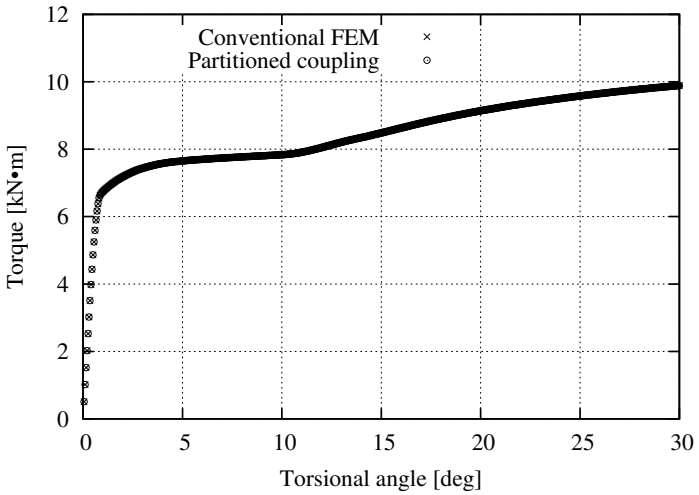

Figure 5: Torsional angle versus torque of the cylindrical specimen model.

in Fig. 4. The vicinity of the notch tip is visualized in the left side. The computed result of torque is shown in Fig. 5. The horizontal axis represents the given torsional angles, while the vertical one does the computed torque. Numerical solution of the partitioned coupling solver agrees well with that of the conventional FEM solver.

Newton–Raphson's convergence property of the conventional FEM solver is shown in Fig. 6. The horizontal axis represents incremental steps, while the vertical one does Newton–Raphson's iteration counts at each incremental step. The convergence property of the partitioned coupling solver is also shown in Fig. 7. Partitioned coupling was suc-

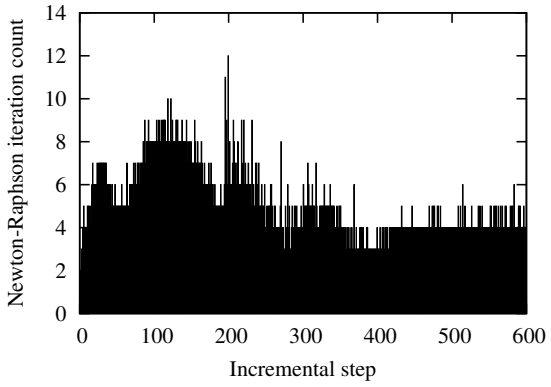

Figure 6: Newton–Raphson iteration counts of the conventional FEM solver.

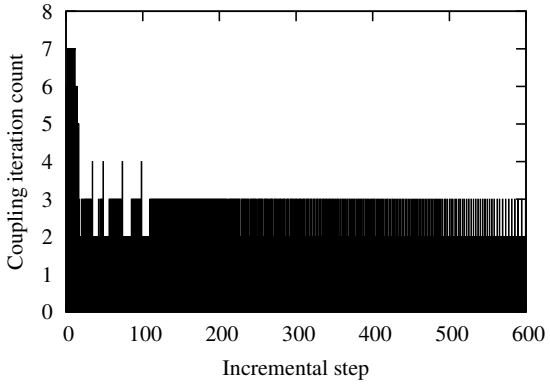

Figure 7: Partitioned coupling iteration counts of the partitioned coupling solver.

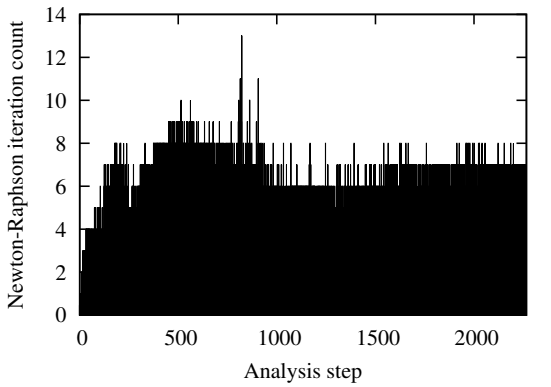

Figure 8: Newton–Raphson iteration counts on the local mesh of the partitioned coupling solver.

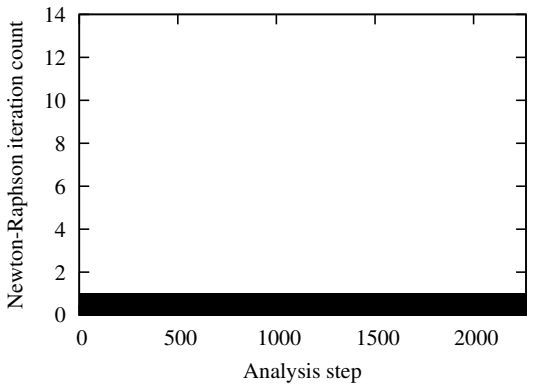

Figure 9: Newton–Raphson iteration counts on the global mesh of the partitioned coupling solver.

cessfully converged in several iterations at every incremental step. Newton–Raphson's convergence properties on the local and global meshes are shown in Fig. 8 and Fig. 9, respectively. Since the form of Fig. 8 seems similar to Fig. 6, it is apparent that the partitioned coupling approach does not degrade Newton–Raphson's convergence property. Newton–Raphson iteration counts on the global mesh are only a few as Fig. 9, because plasticity is not considered on the global mesh. The global domain is modelled as a nonlinear large-deformation elastic body.

4 CONCLUSION

The partitioned coupling method with the limited-memory Broyden method was applied to a cracked model of finite-strain elastoplasticity. A hyperelasticity-based multiplicative decomposition model with Hencky logarithmic strain is used to model finite-

strain elastoplasticity. The cracked model is a cylindrical specimen model with a 60-deg circumferential notch subjected to torsional loading. Finite-strain elastoplasticity is considered on the local mesh, whereas finite-strain elasticity is considered on the global one. The computed result of torque agreed with that of the conventional FEM solver. Partitioned coupling was successfully converged in several iterations at every incremental step. Newton–Raphson iteration counts on the local mesh were similar to those of the conventional FEM solver, which means that the partitioned coupling approach does not degrade Newton–Raphson's convergence property. On the other hand, Newton–Raphson iteration counts on the global mesh were only a few because plasticity is not considered on the global mesh. It was shown that one can utilize two different nonlinear solvers that work together using the partitioned coupling method to solve a problem in which remarkable nonlinearity occurs in a local region.

In the future, a massively parallel finite element method can be applied to the global mesh to analyze real large-scale complicated-shape structures. In addition, nonlinear and complex phenomena such as crack surface contact and crack propagation can be solved. The partitioned coupling method would work more effectively when nonlinearity on the local mesh differs significantly from that on the global mesh.

ACKNOWLEDGMENT

The authors wish to thank IACM for supporting participation in the conference of WCCM XI, ECCM V and ECFD VI.

REFERENCES

[1] Yusa, Y. & Yoshimura, S. Mixed-mode fracture mechanics analysis of large-scale cracked structures using partitioned iterative coupling method. *Comput. Model. Eng. Sci.*, **91** (6), 445–461, 2013.

[2] Minami, S. & Yoshimura, S. Performance evaluation of nonlinear algorithms with line-search for partitioned coupling techniques for fluid–structure interactions. *Int. J. Numer. Meth. Fluids*, **64** (10–12), 1129–1147, 2010.

[3] Kelley, C. T. *Solving Nonlinear Equations with Newton's Method*. Society for Industrial and Applied Mathematics, 2003.

[4] De Souza Neto, E. A., Peric, D. & Owen, D. R. J. *Computational Methods for Plasticity: Theory and Applications* (translated into Japanese by Terada, K. et. al.), Morikita Publishing, 2012.